LSST Controlled Document

Handle: LPM-17

Release Status: Unrestricted – Public Release

The LSST System Science Requirements Document

Version 5.1.1

Author(s):   Zeljko Ivezic and the LSST Science Collaboration

Date: March 24, 2010

Summary: This document defines science-driven requirements for the Large Synoptic Survey Telescope (LSST). It is the governing document for the flow down of requirements for the LSST observatory system including data products.

Document Change Log

Handle: LPM-17

Creation Date: March 24, 2010

Author(s): Zeljko Ivezic and the LSST Science Collaboration

Revision Author(s)	Revision Date	Description of Changes
Zeljko Ivezic and Science Council	March 24, 2010	Updated version 4.3.3 dated Sept 14, 2007

The LSST System Science Requirements Document
v5.1.2, May 5, 2010

1 Introduction

The main purpose of this document is to define science-driven requirements for the data products to be delivered by the Large Synoptic Survey Telescope (LSST). The LSST is envisioned to be a large, wide-field ground based telescope designed to obtain sequential images covering over half the sky every few nights. The current baseline design would allow to do so in two photometric bands every three nights. This baseline design (for details see Appendix A) involves a 3-mirror system with an 8.4 m primary mirror, which feeds three refractive correcting elements inside a camera, providing a 10 deg^2 field of view sampled by a 3 Gigapixel focal plane array. The total effective system throughput (étendue) is expected to be greater than 300 m^2 deg^2, which is more than an order of magnitude larger than that of any existing facility. The survey will yield contiguous overlapping imaging of $\sim$20,000 square degrees of sky in six optical bands covering the wavelength range 320–1050 nm. Detailed simulations that include measured weather statistics and a variety of other effects which affect observations predict that each sky location can be visited about 100 times per year, with 30 sec exposure time per visit.

The range of scientific investigations which would be enabled by such a dramatic improvement in survey capability is extremely broad and is summarized in detail in the LSST Science Book[1]. However, it is not feasible to make an exhaustive study of the scientific requirements appropriate to all of them. To define quantitative science drivers and resulting requirements, we therefore limit our attention in this document to four main science themes:

1. Constraining Dark Energy and Dark Matter

2. Taking an Inventory of the Solar System

3. Exploring the Transient Optical Sky

4. Mapping the Milky Way

Each of these four themes itself encompasses a variety of analyses, with varying sensitivity to instrumental and system parameters. It is our belief that the analyses encompassed by our four science themes fully exercise the technical capabilities of the system, such as photometric and astrometric accuracy and image quality. The working paradigm at this time is that all such investigations will utilize a common database constructed from an optimized observing program. An example of such a program is described in Appendix B.

Below, we include short summaries of the science goals in each of these four theme areas and the assumptions that have been invoked in translating these into the minimum and design specification parameters. This document concludes with Tables of Science Requirements, in which we have integrated the constraints from the different programs.

---

[1]Available from http://www.lsst.org/lsst/scibook

These science requirements are made in the context of what we forecast for the scientific landscape in 2015. Clearly science will not stand still in the intervening time. Using current plans for smaller surveys and precursor projects one may calculate efficiencies and gauge the likely progress on a number of LSST-related scientific frontiers. Some advances in each area will be made, but the LSST remains the ultimate facility for each key area covered in this SRD. Indeed, LSST represents such a large leap in throughput and survey capability that in these key areas the LSST remains uniquely capable of addressing sharply these fundamental questions about our universe.

2   The LSST Science Drivers

The LSST collaboration has identified the aforementioned four science programs as the normative key drivers of the science requirements for the project. Their selection was the result of discussions within the consortium and reflects the input of

- the three National Research Council studies[2] that have endorsed the LSST,

- the report of the LSST Science Working Group (SWG), an independent committee formed by NOAO to represent community interests

- the scientific interests of the partners in the LSSTC

- the physics and astrophysics community.

The SWG report[3] (also known as the Strauss report), the LSST NSF proposal[4], the LSST Dark Energy Task Force report[5], and the LSST Science Book should be consulted for a more detailed discussion of the major scientific advances that can be expected from the construction of a wide-field telescope that is dedicated to repeated, deep, multi-color imaging of the sky.

For each of the four primary science drivers selected by the LSST collaboration, this Section briefly describes the science goals and the most challenging requirements for the telescope and instrument that are derived from those goals (separate documents will deal with the data management requirements[6]). Tables are also provided in the subsequent Section, that integrates the detailed requirements of these four programs. If these requirements are met by the LSST – and indications of the preliminary engineering studies undertaken to date indicate that they can be – then the LSST will not only enable all four of these major scientific initiatives but will also make it possible to pursue many other research programs.

---

[2]Astronomy and Astrophysics in the New Millennium, NAS 2001; Connecting Quarks with the Cosmos: Eleven Science Questions for the New Century, NAS 2003; New Frontiers in the Solar System: An Integrated Exploration Strategy, NAS 2003.

[3]Available as http://www.lsst.org/Science/docs/DRM2.pdf

[4]Available (to LSST) as http://docushare.lsstcorp.org/docushare/dsweb/Get/Document-220

[5]Available as http://www.lsst.org/Science/docs/050617c_deftwp.pdf

[6]The two high-level documents derived from this document and other constraints are the LSST System Requirements Document and the LSST System Architecture Document.

Some examples are described in the LSST Science Book, but the long-lived data archives of the LSST will have the astrometric and photometric precision needed to support entirely new research directions which will inevitably develop during the next several decades.

2.1 Constraining Dark Energy and Dark Matter

Driven by observations, current models of cosmology require the existence of both dark matter and dark energy (DE). One of the primary challenges for fundamental physics is to understand these two major components of the universe. In addition to making a unique map of dark matter structure over half the sky, LSST will probe dark energy in multiple ways, providing cross checks and removal of important degeneracies. The primary DE science drivers for LSST come from a suite of two and three point cosmic shear tomography analyses coupled with galaxy power spectrum and baryon acoustic oscillation (BAO) data, as well as from the use of supernovae as standard candles. Due to its wide area coverage, LSST will be uniquely capable of measuring 7 parameters related to DE: the lowest 6 eigenmodes of the DE equation of state vs. redshift, $w(z)$, and any directional dependence. Combining these probes, LSST will measure the comoving distance as a function of redshift in the redshift range 0.3–3.0 with an accuracy of 1-2%, and separately the growth of cosmic mass structure. A sample of about four billion galaxies with sufficiently accurate photometric redshifts is required. In order to achieve this comoving distance accuracy, the photometric redshifts requirements for this $i < 25$ flux-limited galaxy sample are i) the rms (σ) for error in $(1 + z)$ must be smaller than 0.02, ii) the fraction of 3σ ("catastrophic") outliers must be below 10%, and iii) the bias must be below 0.003. These requirements are primary drivers for the photometric depth of the main LSST survey. In addition, methods for rejecting the majority of those outliers, and for characterizing their effects on the sample, must be developed. The calibration of photometric redshifts and their errors can be a combination of correlation with bright spectroscopic samples and spot-checks with many-band photometric redshift samples. Combining BAO with weak lensing of galaxies can significantly reduce sensitivity to bias systematics.

DE exerts its largest effects at moderate redshift; LSST's redshift coverage will bracket the epoch at which DE began to dominate the cosmic expansion. When combined with Planck CMB data, the LSST data will sharply test models of DE, whether due to new gravitational physics, vacuum energy, or other causes.

2.1.1 Weak Lensing Studies

Weak lensing (WL) techniques can be used to map the distribution of mass as a function of redshift and thereby trace the history of both the expansion of the universe and the growth of structure (see Chapter 14 in the LSST Science Book). These investigations use common deep wide-area multi-color imaging with stringent requirements for the shear systematics in at least two bands and photometry in all bands. These requirements are covered in more detail in the LSST DETF report and references therein.

The shear systematic errors can be mostly corrected by use of foreground stars. The spatially varying PSF within each exposure must be mapped, fit, and corrected. The precision of this correction depends on how many stars are available, and thus depends on the angular scale. The overall scale of the combined errors is set by the requirement of distinguishing models of the origin of DE: unique sensitivity to the cosmic shear power spectrum from arcminute to 100 degree scales and wide redshift range, the ability to probe at least six DE eigenfunctions, and any variation over the sky. This leads to an étendue requirement for *areal coverage times depth* (several billion source galaxies to z=3), as well as photometric precision and wide angular coverage (> 90 deg).

The power of the LSST relative to existing weak lensing surveys derives from its ability to survey much larger areas of the sky to faint limiting surface brightness while maintaining exquisite control of systematic errors in the galaxy shapes. Characterizing dark energy places particularly strong requirements on the total area of sky covered, the depth of the stacked image, the number of revisits to each field, the ellipticity and sampling of the point spread function (PSF), and the choice of filters, which must be suited to allow accurate photometric redshifts to be measured. At least six bands are required. Photometric precision of at least 1% is required, as well as quite accurate calibration of photometric redshifts over the redshift interval $0.3 - 3$.

The scale of residual shear errors should be set by the statistical error floors on the coadded data, not systematics. The two components of statistical shear errors vary oppositely with angular scale. On small angular scales ($<$ few arcminutes) the source galaxy shear error is dominated by the random "shot" noise of the galaxy intrinsic ellipticities (about e=0.3 rms per galaxy) and the finite areal density of source galaxies. On large angular scales the source shear error is dominated by large scale structure cosmic variance. The cross-over point varies with source redshift. For all redshifts in projection, the two errors sum to nearly a constant statistical shear power of 3×10^{-7}, or a source rms residual ellipticity of 0.001, over the range of angular scales for LSST WL science. The residual shear power systematics at all angular scales (*after PSF corrections*) must be less than 30% of the statistical shear power, including correlations between angle bins. To achieve this goal, the residual shear power systematics (after corrections) must be below the statistical errors by a factor of ~3. While the statistical error is uncorrelated with angular scale (as source galaxies are randomly oriented), systematic errors are typically correlated. Statistical errors are reduced when averaged over many exposures and a broad angular band, but systematics do not average down unless they are chopped or vary stochastically from exposure to exposure due to seeing. Thus there are two limiting angular regimes with different methods for reductions of systematics: (1) arcminute scale systematics in the residual PSF ellipticity correlation average down like the number of exposures [further tests are needed for large N], and (2) degree scale residual systematics can be reduced via chopping by dithering and rotating. In both cases further tests are needed to make sure residuals continue to average down to the needed level.

2.1.2 Supernovae

Supernovae (SN) provided the first evidence that the expansion of the universe is accelerating. LSST will be a powerful SN factory (see Chapter 11 in the LSST Science Book). Operating in a standard mode of repeated scans of the sky with images taken every few days and with exposures of 30 seconds, LSST will discover of the order 10^5 Type Ia SN annually. Their mean redshift will be $z \sim 0.45$ with a maximum redshift of ~ 0.7. These data, when combined with priors from other experiments, can constrain the lowest eigenmode of w (*i.e.* the mean value) in the nearby universe to 1% (limited by systematics), and given the dense sampling on the sky, can be used to search for any dependence of w on direction, which would be an indicator of new physics. Some SN will be located in the same direction as foreground galaxy clusters; a measurement of the magnification of the SN will make it possible to model the cluster mass distribution. Core-collapse SN will provide estimates of the star formation rate during the epoch when star formation was changing very rapidly. Longer exposures (10-20 minutes/band) of a small area of the sky could extend the discovery of SN to a mean redshift of 0.7 with some objects beyond $z \sim 1$. The added statistical leverage on the "pre-acceleration" era will narrow the confidence interval on both w and its derivative with redshift.

Spectroscopic follow-up for so many SNe will be impossible. Exploitation of the data from the LSST will require light-curves which are well-sampled both in brightness and color as a function of time. This is essential to the search for systematic differences in supernova populations which may masquerade as cosmological effects as well as for determining photometric redshifts from the supernovae themselves; the development of techniques for determining photometric redshifts from supernova light-curves is currently being pursued by several community groups. Good image quality is required to separate SNe photometrically from their host galaxies. Observations in five photometric bands will be necessary to ensure that, for any given supernova, light-curves in four bands will be obtained (due to the spread in redshift). Absolute band-to-band photometric calibration to 1% is adequate, but the importance of K-corrections to supernova cosmology implies that the calibration of the relative offsets in zero points between filters remains a serious issue, as is stability of the response functions, especially near the edges of bandpasses where the strong emission and absorption features from supernovae makes this more of a problem than for stellar spectra.

2.2 Taking an Inventory of the Solar System

LSST will provide data for millions of small bodies in our Solar System. Previous studies of these objects have led to dramatic changes in our understanding of the process of planet formation and evolution, and the relationship between our Solar System and other systems. These small bodies also serve as large populations of "test particles", recording the dynamical history of the giant planets, revealing the nature of the Solar System impactor population over time, and illustrating the size distributions of planetesimals, which were the building blocks of planets (see Chapter 5 in the LSST Science Book).

The Earth orbits within a swarm of asteroids; some small number of these objects

will ultimately strike the Earth's surface. The U.S. Congress has mandated that by the year 2008, 90% of the near-Earth asteroids (NEAs) with diameters greater than 1 km be discovered and their orbits determined. Impacts of NEAs of this size have the potential to change the Earth's climate and cause mass extinctions, such as the one credited with killing the dinosaurs. A NASA report published in 2003 estimates conservatively that with current search techniques, about 70% of the NEAs with diameters larger than 1 km will have been be cataloged by 2008. This same report quantifies the risk of impacts by smaller bodies, which have the potential of causing significant ground damage, and recommends reduction of the residual hazard by another order of magnitude as a reasonable next goal. Achieving this goal would require discovery of about 90% of the potentially hazardous asteroids (PHAs) down to diameters of about 140 m. While it is unlikely that any other currently planned facility could achieve this goal within a decade or two, modeling suggests that the LSST is capable of finding 84% of the PHAs with diameters larger than 140 m within ten years.

The search for PHAs puts strong constraints on the cadence of observations, requiring closely spaced pairs of observations two or preferably three times per lunation in order to link observations unambiguously and derive orbits. Individual exposures should be shorter than about 1 minute each to minimize the effects of trailing for the majority of moving objects. Because of the faintness and the large number of PHAs and other asteroids that will be detected, LSST must provide the follow-up required to derive orbits rather than relying, as current surveys do, on separate telescopes. The observations should be obtained within ±15 degrees of the Ecliptic. The images should be well sampled to enable accurate astrometry, with absolute accuracy not worse than 0.1 arcsec for sources detected with the signal-to-noise ratio $SNR > 10$. There are no special requirements on filters, although bands such as V and R that offer the greatest sensitivity are preferable. The images should reach a depth of at least 24.5 (5σ for point sources) in the r band in order to probe the ~ 0.1 km size range at main-belt distances. Based on recent photometric measurements of asteroids by the Sloan Digital Sky Survey, the photometry should be better than 1-2% to allow for color-based taxonomic classification.

The LSST can also make a major contribution to mapping Kuiper Belt Objects (KBOs). The orbits of KBOs provide a fossil record of the early history of the solar system; their eccentricities and inclinations contain clues to past perturbations by giant planets. The sizes of the KBOs hold clues to the accretion events that formed them and to their subsequent evolution through collisional grinding, etc. The compositions of KBOs are not identical and are correlated with their dynamical state; the reasons for these differences are not known. Light curves can be used to constrain the angular momentum distribution and internal strengths of the bodies. A more complete sample of KBOs and determination of their properties can assist with selecting targets for future NASA missions. The survey for PHAs can simultaneously provide the joint color-magnitude-orbital distribution for all bright ($r < 24$) KBOs. The 100 or so observations obtained for each bright KBO can be searched for brightness variations, but modeling will be required to determine how well periods can be extracted from observations made at random times. At the very least, it will be possible to determine amplitudes for many thousands of KBOs, and periods can likely

be derived for many of them.

Long exposures would be required to push the detection of KBOs to smaller sizes and reach the erosion-dominated regime in order to study the collisional history of various types of KBOs. KBO science would be greatly amplified if a small fraction of the observing time were devoted to hour-long observations in the ecliptic. This same mode of observation may have applications to the study of variable and transient objects. Apart from exposure time limits, the requirements for the KBO science are similar to the requirements for the detection and orbital determination for other Solar System bodies.

2.3 Exploring the Transient Optical Sky

The LSST will open a new window on the variable sky (see Chapter 8 in the LSST Science Book). Recent surveys have shown the power of variability for studying gravitational lensing, searching for supernovae, determining the physical properties of gamma-ray burst sources, etc. The LSST, with its repeated, wide-area coverage to deep limiting magnitudes will enable the discovery and analysis of rare and exotic objects such as neutron star and black hole binaries; gamma-ray bursts and X-ray flashes, at least some of which apparently mark the deaths of massive stars; AGNs and blazars; and very possibly new classes of transients, such as binary mergers and stellar disruptions by black holes. It is likely that the LSST will detect numerous microlensing events in the Local Group and perhaps beyond. The LSST would provide alerts for concerted monitoring of these events, and open the possibility of discovering planets and obtaining spectra of lensed stars in distant galaxies as well as our own. LSST can also provide multi-wavelength monitoring over time of objects discovered by the Fermi Gamma-ray Space Telescope (formerly GLAST) and the Energetic X-ray Imaging Survey Telescope (EXIST). With its large aperture, the LSST is well suited to conducting a Deep Supernova Search in selected areas. LSST will also provide a powerful new capability for monitoring periodic variables, such as RR Lyrae stars, which can be used to map the Galactic halo and intergalactic space to distances exceeding 400 kpc. Since LSST extends time-volume space a thousand times over current surveys, the most interesting science may well be the discovery of new classes of objects.

Exploiting the capabilities of LSST for time domain science requires large area coverage to enhance the probability of detecting rare events; time coverage, since light curves are necessary to distinguish certain types of variables and in some cases infer their properties (*e.g.* determining the intrinsic luminosity of supernovae Type Ia depends on measurements of their rate of decline); accurate color information to assist with the classification of variable objects; good image quality to enable differencing of images, especially in crowded fields; and rapid data reduction and classification in order to flag interesting objects for spectroscopic and other follow up with separate facilities. Time scales ranging from ∼1 min (to constrain the properties of fast faint transients such as those recently discovered by the Deep Lens Survey) to ∼10 years (to study long-period variables and quasars) should be probed over a significant fraction of the sky. It should be possible to measure colors of fast transients on timescales of a few minutes, and to reach $r \sim 24$ in individual visits. Fast reporting of likely transients to the community is required in order to facilitate followup observations.

2.4 Mapping the Milky Way

The LSST is ideally suited to answering two basic questions about the Milky Way Galaxy: What is the structure and accretion history of the Milky Way? What are the fundamental properties of all the stars within 300 pc of the Sun? (see Chapters 6 and 7 in the LSST Science Book).

Standard models posit that galaxies form from seeds planted by the Big Bang with accretion over time playing a significant role in determining their structure. Detailed study of the Milky Way can provide rigorous tests of these ideas, and the LSST will be able to map the 3-D shape and extent of the halo of our Galaxy. Specifically, the LSST will detect F turn-off stars to distances of 200 kpc; isolate stellar populations according to color; and determine halo kinematics through measurement of proper motions at distances exceeding 10 kpc. The LSST dataset can be used to identify streams of stars in the halo that are thought to provide a fossil record of discrete accretion events. The LSST in its standard surveying mode will be able to detect RR Lyrae variables and classical novae at a distance of 400 kpc and hence can explore the extent and structure of our own halo out to half the distance to the Andromeda Galaxy. The proper motions and photometric parallaxes for these stars can be used to characterize the properties of the dark matter halo in which the Milky Way is embedded. The LSST will survey a significant fraction of the Galactic plane, including the Galactic center, and will obtain unprecedented data for studies of star-forming regions.

Is our solar system with its family of planets unique? Or are there many more that contain Earth-like planets within the so-called habitable zone? How do solar systems form? Detailed exploration of our local neighborhood is key to answering these questions. The LSST will obtain better than 3σ parallax measurements of hydrogen-burning stars to a distance of 300 pc and of brown dwarfs to tens of parsecs. These measurements will provide basic information on candidate stars that merit further study in the search for companions, including planets. Residuals from the fits for position, proper motions, and parallax will be searched for the signature of Keplerian motion to identify stars and brown dwarfs with companions and provide fundamental estimates of the mass of the primaries. LSST data will be used to determine the initial mass functions for low-mass stars and sub-stellar mass objects and to test models of brown dwarf structure. The age of the Galactic disk can be inferred from white dwarf cooling curves.

Key requirements for mapping the Galaxy are large area coverage; excellent image quality to maximize the accuracy of the photometry and astrometry, especially in crowded fields; photometric precision of at least 1% to separate main sequence and giant stars; stringent astrometric accuracy to enable parallax and proper motion measurements; and dynamic range that allows measurement of astrometric standards at least as bright as r = 15. In order to probe the halo out to distances of 100 kpc using large numbers of main sequence stars, the total depth (5σ for unresolved sources) has to reach $r \sim 27$ (assuming 5% photometry in the r band at $r = 25.5$). To study the metallicity distribution of stars in the Sgr tidal stream and other halo substructures at distances out to at least $\sim$40 kpc, the coadded depth in the u band has to deliver 5% photometry at $u \sim 24.5$. In order to constrain tangential velocity

at a distance of 10 kpc to within 10 km/s with the most luminous main-sequence stars (low-metallicity blue turn-off stars with $M_r = 5.5$), the proper motion accuracy has to be at least 0.2 mas/yr at $r = 20.5$ (1σ per coordinate). The same requirement follows from the decision to obtain the same proper motion accuracy as Gaia at its faint end ($r \sim 20$). The LSST will then represent an "extension" of Gaia astrometric measurements to 4 magnitudes greater depth. In order to produce a complete sample of the solar neighborhood stars out to a distance of 300 pc (the thin disk scale height), with 3σ or better geometric distances, parallax measurements accurate to 1 mas (1σ) are required for stars with $M_r = 15$. To obtain 3σ or better geometric distances for T9/Y0 brown dwarfs with $z - y$ colors measured with 10σ or better precision (in coadded data), parallax measurements for sources detected only in y band visits at 10σ significance must have an accuracy of 6 mas (1σ).

In summary, these requirements imply that the LSST will enable studies of the distribution of numerous main-sequence stars beyond the presumed edge of the Galaxy's halo, of their metallicity distribution throughout most of the halo, and of their kinematics beyond the thick disk/halo boundary, and will obtain direct distance measurements below the hydrogen-burning limit for a representative thin-disk sample.

3 Detailed Description of Science Requirements

The purpose of this Section is to lay out a common set of science requirements necessary to achieving a set of concrete scientific measurements, of specified accuracy, in the four main science areas described above. It will serve as the primary starting point for deriving engineering requirements to be placed upon the various technical subsystems that comprise the LSST. Note that some of these requirements are not fully independent of the existing baseline design (see Appendix A), and of realities such as seeing and sky brightness distribution at the selected site (Cerro Pachón in Chile). While different science programs require broadly consistent datasets, the adopted values represent the most stringent requirements from the previous section.

3.1 The Definitions of Specified Parameters

For each quantity specifying a requirement, we identify two values: a *minimum specification*, and a *design specification.*

The minimum specification shall represent the minimum capability or accuracy required of the system in order to achieve its scientific aims. If the design analysis clearly demonstrates that a minimum specification requirement cannot be met, the Science Council will reevaluate the science drivers that led to the specification, estimate the scientific impact of the failure to meet the specification, and report the findings to the Project Director and Project Manager.

The design specification represents the system design point and will be used as the basis for developing engineering tolerances. At the time this document is written, we believe that the design specification should be achievable in the context of the existing baseline concept for the LSST. However, as development proceeds, it is conceivable that there may be some change in capability away from these values.

In some cases, *stretch goals* are specified. These are desirable system capabilities which will enhance scientific return if they can be achieved. Stretch goals are to be pursued if they do not significantly increase cost, schedule or risk. To avoid complication and ambiguity, we do not list these in every instance; it remains understood that wherever improved capability is easily achievable, it should be pursued. Situations where enhanced capability beyond the design specification compromises cost, schedule, or other system parameters must be evaluated on a case-by-case basis to decide whether they make sense in the context of the whole system. In addition to numerical requirements, a brief reference to the science program that places the strongest constraints is also provided.

3.2 Distinction between Single Image Specifications and the Full Survey Performance

Detailed simulations show that the LSST will be capable of obtaining over 200,000 10 deg^2 images per year, assuming 30 sec total exposure per image and realistic observing conditions for Cerro Pachón. For each of these images, a decision involving at least three free

parameters (position on the sky and filter; assuming fixed exposure time and position angle of the field of view) must be made. With a simplifying assumption of only 2,000 allowed sky positions (*i.e.* a fixed grid of 10 deg^2 field centers tiling an area of 20,000 deg^2) and 5 filters, there will be over 10^{10} different ways to execute the LSST observations over its projected 10-year lifetime. Hence, the optimization of LSST observing strategies is a formidable problem that requires significant additional analysis. For this reason, only weak constraints for observing cadence are listed here (though integral quantities such as total depth and sky coverage are specified). The required properties of individual images (also known as *visits*, consisting of two co-added, back-to-back exposures), however, are specified in detail because they directly constrain the capabilities of the hardware and software systems. The detailed error budget distribution between the hardware and software systems is not considered here and will be addressed in a separate documents (the LSST System Requirements Document and the LSST System Architecture Document). As a general principle, the measurement errors for fundamental quantities, such as astrometry, photometry and image size, should not be dominated by algorithmic performance.

3.3   Single Image Specifications

The fundamental image properties specified in this section are

- Bandpass characteristics

- Image depth (attained magnitude at some fiducial signal-to-noise ratio)

- Image quality (size and ellipticity)

- Astrometric accuracy

- Photometric accuracy

There are several factors that increase the complexity of these specifications. Many of the image properties depend on quantities such as zenith angle (airmass), wavelength, sky brightness, relative positions on the sensor and within the field of view, and attained signal-to-noise ratio. Most of these quantities are actually distributions, and can be specified by a single number only in special cases, such as that of a perfect Gaussian distribution (with zero mean).

We address these complexities as follows. For quantities with strong wavelength dependence, requirements are specified in each band. Where relevant, fiducial seeing and airmass are specified. For quantities with a strong dependence on the signal-to-noise ratio (SNR), requirements are specified at the *bright end*, defined here as the magnitude range between 1 mag and 4 mag fainter than the saturation limit (full well) in a given bandpass. Assuming that the faint end of this range corresponds to $r = 20$, and that 5σ depth is achieved at $r = 24.5$, the photon statistics limits on photometric and astrometric accuracy ($SNR \sim 200$) are 5 millimag and 4 milliarcsec for a fiducial delivered seeing of 0.7 arcsec. Both of these limits are sufficiently small as to allow the required overall photometric and

11

astrometric accuracy described below (which include effects such as sky brightness and in-strumental noise, as well as various calibration uncertainties). About 1% of all the sources detected in a typical LSST image will be brighter than $r = 20$. At this magnitude, the sur-face densities of galaxies and high-Galactic-latitude stars are similar: about 1000 per square degree (implying a typical nearest-neighbor distance for stars of the order of 1 arcmin).

We define "FWHM" as *the full width at half maximum*, and "rms" as *the root-mean-square scatter*. For a one-dimensional Gaussian distribution, FWHM = 2.35 rms.

3.3.1 Filter Set Characteristics

The filter complement (Table 1) is modeled after the Sloan Digital Sky Survey (SDSS) system because it has demonstrated success in a wide variety of applications such as pho-tometric redshifts of galaxies, separation of stellar populations, and photometric selection of quasars.

Quantity	Design Spec	Minimum Spec	Stretch Goal
Filter complement	ugrizy	ugrizy	ubgrizy

Table 1: The filter complement.

The extension of the SDSS system to longer wavelengths (the y band at ~ 1 μm) is mandated by the increased effective redshift range achievable with the LSST due to deeper imaging, and the desire to study regions of the Galaxy that are obscured by interstellar dust. The optimal wavelength range for the y band is still under investigation. A narrow, blue b filter may increase the photometric redshift accuracy, but the quantitative effects of its addi-tion are also under investigation. The addition of the u band will improve the robustness of photometric redshifts of galaxies and stellar population separation, will enable quasar color selection and stellar metallicity estimates, and will provide significant additional sensitivity to star formation histories of detected galaxies (*e.g.* GALEX bands are redshifted to the u band for galaxies at redshifts of about 1, close to the median redshift for galaxies detectable in deep LSST images). The current design of the bandpasses is illustrated in Appendix C.

The Number of Filters Used in a Night
The number of filters, Nfilters, to be used on the same night is equivalent to the number of filters that can be simultaneously housed within the camera. It is assumed that any other filter from the filter complement can be inserted during the daytime, even on the shortest winter days.

Specification: The number of filters available at any given time is specified as Nfilters (Table 2).

Quantity	Design Spec	Minimum Spec	Stretch Goal
Nfilters	5	3	6

Table 2: The number of filters that can be housed simultaneously within the camera.

Specification: The maximum time allowed to switch filters already present inside the camera is specified as TFmax (Table 3).

Quantity	Design Spec	Minimum Spec	Stretch Goal
TFmax (min)	2	10	1

Table 3: The maximum time, in minutes, allowed to switch filters already present inside the camera.

The ability to rapidly switch active filters will allow more useful color measurements of fast transients.

Filter Out-of-Band Constraints
Specification: Beyond the wavelengths where the transmission curve (including hardware and atmosphere) decreases to below 0.1% of its peak value for the first time, the mean transmission in any 10nm interval must be less than Fleak % of the peak value, and the integrated transmission at those wavelengths must be below FleakTot % of the overall transmission (Table 4).

Quantity	Design Spec	Minimum Spec	Stretch Goal
Fleak (%)	0.01	0.02	0.003
FleakTot (%)	0.05	0.1	0.02

Table 4: Filter Out-of-Band Constraints (transmission in % of the peak value in any 10nm interval beyond one FWHM of the central wavelength, Fleak, and total transmission out of band, FleakTot).

This requirement assures reasonable photometric accuracy for objects with extreme colors. For example, for a source with the color $u - i = 5$, the effect of a u band red leak confined to the i band (*e.g.* see Appendix C) is limited to a 0.05 mag bias in the u band measurement (<0.01 mag for sources bluer than $u - i = 3$).

The temporal change of bandpasses (due to aging of the filters, changes in reflectivity of coatings, *etc.*) must be sufficiently small to enable the required photometric calibration accuracy (specified below, see §3.3.4).

3.3.2 Image Depth and the Minimal Exposure Time

An *exposure* means a single readout of the camera (one of the two back-to-back exposures designed for cosmic ray rejection that together represent a *visit* to a target field). Image properties, such as depth (attained magnitude for point sources at some fiducial SNR, here taken to be 5), **are defined per visit** (not per exposure), and assume optimal count extraction algorithms (e.g. point-spread-function magnitudes). The image depth depends on total exposure time, bandpass, delivered image quality (dominated by atmospheric seeing as per image quality requirement), the sky brightness and its spatial structure, and the

system efficiency. For a given exposure time, fiducial seeing, and sky brightness, the required image depth is an indirect constraint on the system's efficiency (assuming a fixed effective primary mirror diameter).

The overall image depth distribution

Specification: The distribution of the 5σ (SNR=5) detection depth for point sources for all the exposures in the r band will have a median not brighter than D1 mag, and no more than DF1 % of images will have a 5σ depth brighter than Z1 mag. The implication of many exposures only formally violates the paradigm of a single image specification in this section; this requirement can be understood as a probability distribution for the attained depth (DF1 is the fraction not of all exposures, but of those in the r band in good seeing on photometric dark nights and close to the zenith, corrected to the fiducial parameters listed in Table 5).

Quantity	Design Spec	Minimum Spec	Stretch Goal
D1 (mag)	24.7	24.5	24.8
DF1 (%)	10	20	5
Z1 (%)	24.4	24.0	24.6

Table 5: Single image depth in the r band (SNR=5 for point sources). The D1 and Z1 values are expressed on the AB magnitude scale and assume a source with spectral energy distribution F_ν=constant, fiducial seeing of 0.7 arcsec (FWHM), fiducial dark sky brightness of 21 mag/arcsec^2, airmass of 1.0, and a total exposure time of 30 sec. The sky brightness is a conservative estimate corresponding to solar maximum. Solar minimum value may be 0.3-0.4 mag fainter, resulting in $\sim$0.2 mag deeper data. On the other hand, about $\sim$0.2 mag loss of depth is expected for data obtained at airmass of 1.4 (mostly due to seeing degradation).

For a given exposure time and observing conditions, the required depths primarily constrain the effective primary mirror diameter and overall (hardware + atmosphere) system throughput. The chosen exposure time per visit (2×15 sec) is a result of the survey optimization and satisfies both the required final coadded depth, single visit depth, and the revisit time if the effective primary mirror diameter is 6.5m. The single visit depth is driven by transient sources and motion measurements (for both Solar System objects and stellar proper motions) and the coadded depth is driven by the required number of galaxies for cosmological studies (see § 3.4).

The variation of the image depth (throughput) with bandpass

Specification: The median 5σ (SNR=5) detection depth for point sources in a given band will not be brighter than DB1 mag (Table 6).

The science drivers described in §2 and the corresponding image depths listed in Table 6 have motivated the baseline design parameters listed in Appendix A. The assumed

Design spec.	u	g	r	i	z	y
DB1 (mag)	23.9	25.0	24.7	24.0	23.3	22.1

Minim. spec.	u	g	r	i	z	y
DB1 (mag)	23.4	24.6	24.3	23.6	22.9	21.7

Stretch goal	u	g	r	i	z	y
DB1 (mag)	24.0	25.1	24.8	24.1	23.4	22.2

Table 6: Specifications for the single visit depth (DB1) as a function of bandpass (the r-band value is identical to that listed in Table 5), assuming 2×15 sec exposures, a source with spectral energy distribution F_ν=constant, airmass of 1.0, the r-band fiducial seeing of 0.7 arcsec (FWHM), and the r-band sky brightness of 21 mag/arcsec^2 (both seeing and sky brightness are converted to the appropriate band using standard expressions, as implemented in the LSST Exposure Time Calculator).

bandpasses are illustrated in Appendix C. Note that there is no requirement that exposure time be same for all the bands.

If delivered system throughput would result in brighter limiting magnitudes for the nominal conditions, the required DB1 values could be maintained by increasing the integration time. For example, to account for 0.2 mag of loss in limiting depth (equivalent to about 30% loss of throughput), the required additional survey time is about half a year for the u and g bands, and about 1 year for other bands, for a 10-year survey (assuming the time allocation per band discussed in § 3.4). However, while such strategy would deliver the required coadded survey depth, it would have a negative impact on the single visit depth and time sampling frequency. The system throughput should never drop below values needed to meet minimum specifications for image depths listed in Table 6.

The variation of the image depth over the field of view
Specification: For an image representative of the median depth (*i.e.* with the 5σ detection depth of D1 mag), the depth distribution over individual devices will have no more than DF2 % of the sample brighter by Z2 mag than the median depth (Table 7).

Quantity	Design Spec	Minimum Spec	Stretch Goal
DF2 (%)	15	20	10
Z2 (mag)	0.2	0.4	0.2

Table 7: Image depth variation over the field of view. These values apply to all bands.

While the depth depends on the delivered image quality, the implied requirements are less stringent than the direct requirements on the image quality variation over the field of view specified below. The primary purpose of these image depth requirements is to define allowed variation in detector sensitivity.

The Minimum Exposure Time

Specification: The shortest possible exposure time will not be longer than ETmin seconds (Table 8).

Quantity	Design Spec	Minimum Spec	Stretch Goal
ETmin (sec)	5	10	1

Table 8: The minimum exposure time (in seconds).

The minimum exposure time limits the ability to study fast temporal changes in brightness and position. The required specification will enable sampling of time scales three times shorter than the nominal exposure time. As an added benefit, it will enable an extension of the saturation limit $\sim$1 mag brighter than with the nominal exposures. Note that the requirement on relative photometric accuracy specified in Table 14 also applies to these shorter exposures.

3.3.3 The Delivered Image Quality

The delivered image quality depends on atmospheric seeing and distortions introduced by the system. It can be parametrized by the equivalent Gaussian width (see below) and the ellipticity of the delivered PSF. The deviations of the image profile from the implied Gaussianity are parametrized by the radii enclosing specified fractions of the total energy (light).

The weak lensing studies are particularly sensitive to the delivered image quality (other science programs are only indirectly affected, *e.g.* through the dependence of the image depth on image size). As there is no particular threshold to be achieved in the plausible 0.5–0.9 arcsec range, the benefit is a monotonic function of improvements in delivered image quality.

The delivered image size distribution

The delivered image size, hereafter "delivered seeing" (as opposed to atmospheric seeing), is expressed using the "equivalent Gaussian width" computed from

$$\text{seeing} = 0.663 \, \text{pixelScale} \, \sqrt{n_{eff}} \, \text{arcsec.} \tag{1}$$

Here pixelScale is the pixel size in arcsec (0.2 for the baseline design) and n_{eff} is the effective number of pixels computed from

$$n_{eff} = \frac{(\sum f_i)^2}{\sum f_i^2}, \tag{2}$$

where f_i is the image intensity (*i.e.* the sum is over a bright star). In the limit of a perfect single Gaussian profile, the seeing computed using these expressions is equal to the FWHM ($n_{eff} = 2.27 \, (\text{seeing/pixelScale})^2$ for a single Gaussian). Note that this approach is insensitive to the detailed image profile, and accounts for the fact that atmospheric seeing cannot be described by a single Gaussian at the required level of accuracy ($\sim$1%).

16

The image size is specified for three values of fiducial atmospheric seeing: 0.44, 0.60 and 0.80 arcsec. These values are chosen as the three quartiles of the seeing distribution measured at the Cerro Pachón site using DIMM at 500 nm, and corrected using an outer scale parameter of 30 m. The atmospheric seeing distribution at the Cerro Pachón site is illustrated in Appendix D.

Specification: The delivered seeing distribution across the field of view will have a median not larger than S1 arcsec, with no more than SF1 % of images exceeding SX times S1 arcsec (Table 9).

Quantity	Design Spec	Minimum Spec	Stretch Goal
S1 (0.44)	0.56	0.59	0.53
S1 (0.60)	0.69	0.72	0.67
S1 (0.80)	0.87	0.89	0.85
SF1 (%)	10	10	5
SX	1.1	1.2	1.1

Table 9: The delivered seeing distributions for three fiducial values of atmospheric seeing (arcsec). These values apply to the r and i bands.

The required image size is derived by assuming that the delivered image quality will be dominated by atmospheric seeing effects and not by the system. The design specification values reflect an error budget of 0.35 arcsec (for both telescope and camera, and including static and dynamic errors), which is added in quadrature. The minimum specification and stretch goal are computed using error budgets of 0.4 and 0.3 arcsec, respectively. The system contribution to the delivered image quality should not exceed 0.4 arcsec in any other band.

The above design specification for the image quality requires that, for the median atmospheric seeing, the system contribution to the delivered image quality never exceeds 15%. This requirement should be fulfilled irrespective of the airmass, which limits the seeing degradation due to hardware away from the zenith (e.g. due to gravity load).

Specification: The allowed seeing error budget due to system at airmass=2 is SXE arcsec (Table 10).

Quantity	Design Spec	Minimum Spec	Stretch Goal
SXE	0.52	0.59	0.45

Table 10: The image quality error budget due to system at airmass=2 (arcsec).

Assuming that the atmospheric seeing increases with airmass, X, as $\propto X^{0.6}$, the design specification for the allowed error budget due to the system (15% degradation in image quality) is defined at airmass of 2 and for the median seeing conditions (0.91 arcsec at $X = 2$). The minimum specification and the stretch goal are computed by scaling the design specification by 0.3/0.35 and 0.4/0.35, respectively, in analogy with specifications for the S1 parameter (see Table 9).

The Image Sampling
  Specification: The pixel size will be smaller than pixSize arcsec (Table 11).

Quantity	Specification
pixSize	0.22

Table 11: The maximum pixel size (arcsec) to enable proper image sampling.

The pixel size must be smaller than the first quartile of the delivered image size distribution (0.56 arcsec) divided by 2.5. This coefficient is motivated by the need to sample the point-spread function properly in the delivered images.

The seeing spatial profile
  Specification: For a fiducial delivered seeing of 0.69 arcsec (S1 from Table 9 for the median atmospheric seeing), at least 80% of the energy will be encircled within a radius of SR1 arcsec, at least 95% of the energy will be encircled within SR2 arcsec, and at least 99% of the energy will be encircled within SR3 arcsec (Table 12).

Quantity	Design Spec	Minimum Spec	Stretch Goal
SR1 (arcsec)	0.74	0.80	0.70
SR2 (arcsec)	1.20	1.31	1.14
SR3 (arcsec)	1.66	1.81	1.59

Table 12: The spatial profile (shape) for delivered seeing. These values apply to all the bands, as they are defined for a fiducial delivered seeing. For a different fiducial seeing, the SRx/seeing ratio, *i.e.* the *shape* of the delivered image, must be preserved.

The specified values were computed using a double-Gaussian profile that is a good description of both typically-observed seeing profiles and that expected for Kolmogorov turbulence

$$p(x) = G(0, \sigma) + 0.1\, G(0, 2\sigma), \tag{3}$$

where $G(\mu, \sigma)$ is a two-dimensional Gaussian. For this profile, n_{eff} is 31% larger than for a single Gaussian with the same FWHM. For a seeing of 0.69 arcsec described by this profile, the radii enclosing 80%, 95% and 99% of the energy are 0.67, 1.09, and 1.51 arcsec, respectively. Note that it would be grossly incorrect to assume that the seeing can be described by a single Gaussian, as the corresponding radii are 0.52, 0.71, and 0.89 arcsec.

The design specifications were determined by multiplying the above radii by 1.1, and by 1.2 for the minimum specifications. For the stretch goal specifications, the multiplication factor is 1.05. These requirements limit the deviations from the above canonical profile, and in particular, the amount of power in the expected power-law wings, due to the system. The power-law wings observed for free atmospheric seeing have a much smaller amplitude (~10 times, relative to the central intensity) than the upper limit implied by the above requirements.

The image ellipticity distribution

The image ellipticity is defined as $e = (\sigma_{maj}^2 - \sigma_{min}^2)/(\sigma_{maj}^2 + \sigma_{min}^2)$, where σ_{maj}^2 and σ_{min}^2 are, respectively, the 2nd moments of the best fit elliptical double Gaussian. The best fit elliptical Gaussian is used so as to minimize issues of truncation of intensity sums in noisy data. A double Gaussian is specified for consistency with the image size specifications above (the two components are assumed to have the same ellipticity and the same orientation).

Specification: For a delivered seeing of 0.69 arcsec, in a field with a zenith distance of at most 10 degrees, the ellipticity distribution across the field of view for unresolved sources will have a median not larger than SE1, with no more than EF1 % of images exceeding the ellipticity of SE2 (Table 13).

Quantity	Design Spec	Minimum Spec	Stretch Goal
SE1	0.04	0.05	0.03
EF1 (%)	5	10	5
SE2	0.07	0.1	0.05

Table 13: These values apply to the r and i bands.

These values are motivated by observations showing that the ellipticity induced by atmospheric turbulence in a 10-second exposure in 0.69 arcsec will be in the range 0.01-0.02. The specification is set such that the telescope+camera system does not contribute appreciably to the ellipticity beyond the natural limit set by the atmosphere (e.g. tracking errors, jitter in the telescope). This specification does not by itself address weak lensing systematics, because there are schemes for removing the influence of an anisotropic PSF on the observed shapes of galaxies. However, it is known that these schemes leave smaller residuals if initially given isotropic PSFs to begin with, hence the specification that the telescope+camera not greatly degrade the natural limit. The overall image PSF ellipticity distribution is further discussed in Section 3.4 (see Table 26).

3.3.4 Photometric Quality

The photometric accuracy is specified through requirements on relative photometry (repeatability), the system stability across the sky, color zero-points, and the transfer to a physical flux scale (*i.e.* calibration onto the AB magnitude scale).

A broad-band photometric system, such as LSST, aims to deliver calibrated in-band flux

$$F_b = \int F_\nu(\lambda)\phi_b(\lambda)d\lambda, \tag{4}$$

where $F_\nu(\lambda)$ is specific flux of an object *at the top* of the atmosphere and $\phi_b(\lambda)$ is the normalized system response for the given band (the λ^{-1} term reflects the fact that CCDs are photon-counting devices)

$$\phi_b(\lambda) = \frac{\lambda^{-1}S_b(\lambda)}{\int \lambda^{-1}S_b(\lambda)d\lambda}. \tag{5}$$

19

Here, $S_b(\lambda)$ is the overall atmosphere + system throughput

$$S_b(\lambda) = S_b^{sys}(\lambda) \times S_b^{atm}(\lambda). \tag{6}$$

Traditionally, the in-band flux is reported on a magnitude scale, and here we adopt AB magnitudes defined as

$$m_b = -2.5 \log_{10} \left(\frac{F_b}{3631 \text{ Jy}} \right). \tag{7}$$

In order to interpret photometric measurements at the error level specified below ($<1\%$), both $S_b^{sys}(\lambda)$ and $S_b^{atm}(\lambda)$ must be known with sufficient precision. Experience with precursor surveys, such as SDSS, suggest that the dependence of both functions on wavelength have to be directly measured to break the 1% photometric error barrier (especially for sources with complex spectral energy distributions, such as supernovae). While the individual normalizations of $S_b^{sys}(\lambda)$ and $S_b^{atm}(\lambda)$ are *not* required (c.f. eq. 5) to interpret measurements using eq. 4, the flux scale (calibration) errors affect the reported values of F_b (i.e. m_b). Therefore, for each photometric measurement both F_b and $\phi_b(\lambda)$ will be reported, together with their estimated uncertainties. These two quantities will capture fundamental information included in LSST measurements, and will enable accurate transformation of F_b to systems with similar $\phi_b(\lambda)$ when the source spectral energy distribution is known or assumed. In particular, corrections to some standardized "average" LSST system, $\phi_b^{std}(\lambda)$, will be defined during the commissioning period for the most relevant spectral energy distributions (such as main sequence stars and normal galaxies).

The requirements for photometric calibration accuracy are specified using the following error decomposition (valid in the limit of small errors)

$$m_{cat} = m_{true} + \sigma + \delta_m(x, y, \phi, \alpha, \delta, SED, t) + \Delta_m, \tag{8}$$

where m_{true} is the true magnitude defined by eqs. 4 and 7, m_{cat} is the cataloged LSST magnitude, σ is the random photometric error (including random calibration errors and count extraction errors), and Δ_m is the overall (constant) offset of the internal survey system from a perfect AB system (the six values of Δ_m are equal for *all* the cataloged objects). Here, δ_m describes the various systematic dependencies of the internal zeropoint error around Δ_m, such as position in the field of view (x, y), the normalized system response (ϕ), position on the sky (α, δ), and the source spectral energy distribution (SED). Note that the average of δ_m over the cataloged area is 0 by construction.

This error decomposition decouples "internal absolute" calibration (i.e. producing an internally consistent system by minimizing δ_m), from that of "external absolute" calibrations (i.e. determining the six *ugrizy* Δ_m values for the LSST survey). Furthermore, the deviation of the LSST system from a perfect AB system, Δ_m, can be expressed relative to a fiducial band, say r,

$$\Delta_m = \Delta_r + \Delta_{mr}. \tag{9}$$

The motivation for this separation is twofold. First, Δ_{mr} can be constrained by considering the colors (spectral energy distributions) of objects, *independently from the overall*

20

flux scale (this can be done using both external observations and models). Second, there are few science programs that crucially depend on knowing the "gray scale" offset, Δ_r, at the 1-2% level. On the other hand, knowing the "band-to-band" offsets, Δ_{mr}, with such an accuracy is *critically important* for many applications (e.g., photometric redshifts of galaxies, type Ia supernovae cosmology, testing of stellar and galaxy SED models).

The photometric repeatability (relative photometry)
   Specification: The rms of the unresolved source magnitude distribution around the mean value (repeatability) will not exceed PA1 millimag (median distribution for a large number of sources). No more than PF1 % of the measurements will deviate by more than PA2 millimag from the mean (Table 14).

Quantity	Design Spec	Minimum Spec	Stretch Goal
PA1 (millimag)	5	8	3
PF1 (%)	10	20	5
PA2 (millimag)	15	15	10

Table 14: The specifications for photometric repeatability. The listed values apply to the g, r and i bands. The PA1 and PA2 values in the u, z and y bands may be 50% larger.

   This requirement, defined for bright, unresolved sources (*i.e.* those whose measurements are not dominated by photon statistics, see § 3.3), specifies the distribution of random photometric errors, σ, and constrains both the repeatability of extracting counts from images and the ability to monitor (or model) the changes in normalized system response (ϕ). In practice, multiple visits will be used to compute the photometric rms for each individual star in each bandpass and then study its dependence on position on the sky and on the camera, stellar color, brightness, time, etc.
   The specified values are driven by the photometric redshift accuracy, the separation of stellar populations, detection of low-amplitude variable objects (such as eclipsing planetary systems), and the search for systematic effects in type Ia supernova light-curves. To verify that this requirement is fulfilled, samples of predominantly non-variable stars will have to be selected using appropriate color selection. Note that is sufficient to have only two observations to diagnose that this requirement is not fulfilled.

The spatial uniformity of photometric zeropoints
   Specification: The distribution width (rms) of the internal photometric zero-point error (the system stability across the sky) will not exceed PA3 millimag, and no more than PF2 % of the distribution will exceed PA4 millimag (Table 15).
   This requirement on the distribution of $\delta_m(x, y, \phi, \alpha, \delta, SED, t)$ primarily constrains the stability of the internal photometric system across the sky.
   The specified requirements are driven by the photometric redshift accuracy, the separation of stellar populations, and the accuracy of inter-comparing distance moduli from

Quantity	Design Spec	Minimum Spec	Stretch Goal
PA3 (millimag)	10	15	5
PF2 (%)	10	20	5
PA4 (millimag)	15	20	15

Table 15: The specifications for the spatial uniformity of photometric zeropoints. The values for PA3 and PA4 may be somewhat worse in the u band (but not by more than a factor of two).

different supernovae. These requirements apply to *both* the bright and faint ends and constrain the non-linearity of the flux scale. To verify that these requirements are fulfilled, samples of standard stars may be needed (an alternative is to track the shifts of morphological features in color-color diagrams). Note that these requirements also place an upper limit on various systematic errors, such as, for example, a correlation of internal photometric zero-point error with the position on a sensor, and within the field of view.

The band-to-band (flux ratio) photometric calibration
   Specification: The absolute band-to-band zero-point transformations (color zero-points, *e.g.* for constructing the spectral energy distribution, SED) for main-sequence stars must be known with an accuracy of PA5 millimag (Table 16).

Quantity	Design Spec	Minimum Spec	Stretch Goal
PA5	5	10	3
PA5 (with u)	10	15	5

Table 16: The accuracy of color zero-points (in millimag). The second row applies to colors constructed using the u band photometry.

   These requirements on Δ_{mr} are primarily driven by the desired accuracy of photometric redshift estimates. Note that an overall stable gray error in the absolute calibration of the system (Δ_r) does not have an impact on the above requirements. Such an error is specified next.

The overall external absolute photometry
   Specification: The LSST photometric system must transform to a physical scale (*e.g.* AB magnitude scale) with an accuracy of PA6 millimag (Table 17).

Quantity	Design Spec	Minimum Spec	Stretch Goal
PA6	10	20	5

Table 17: The accuracy of photometric system transformation to a physical scale (in millimag).

The requirements on Δ_r are driven by the accuracy of absolute determination of quantities such as luminosity and asteroid size for objects with well determined distances. Note that the internal band-to-band transformations, Δ_{mr}, are required to be much more accurate as they may be calibrated and controlled by other means, and are not sensitive to errors in overall flux scale of photometric calibrators.

Further notes on photometry

The photometry of resolved sources of moderate size (effective radius $\leq$10 arcsec) must have comparable quality (not worse than a factor of 2 in an rms sense, with the same fraction of sources in the distribution tails, as per above requirements) to unresolved stellar sources. The photometric measurements for resolved sources (galaxies) have to include several standard magnitudes, such as Petrosian magnitudes, as well as appropriate model magnitudes.

It is noteworthy that the technical aspects of how the required photometric precision and accuracy will be achieved (*e.g.* calibration schemes, flat-field determination, corrections for atmospheric effects) are purposely left out of this discussion as they belong to the Engineering Requirements Documents; for example, an all-sky cloud camera or new software algorithms (e.g. self-calibration, pioneered as *übercalibration* by SDSS) may be needed to achieve the required photometric accuracy. The same approach is taken when specifying astrometric requirements, described next.

3.3.5 Astrometric Quality

The astrometric requirements are defined for bright unresolved sources (*i.e.* those whose measurements are not dominated by photon statistics, see § 3.3). The astrometric accuracy is specified through requirements on relative astrometry (repeatability) and absolute astrometry.

The relative astrometry

Specification: The rms of the astrometric distance distribution for stellar pairs with separation of D arcmin (repeatability) will not exceed AMx milliarcsec (median distribution for a large number of sources). No more than AFx % of the sample will deviate by more than ADx milliarcsec from the median. AMx, AFx, and ADx are specified for D=5, 20 and 200 arcmin for x= 1, 2, and 3, in the same order (Table 18).

The three selected characteristic distances reflect the size of an individual sensor, a raft, and the camera. The required median astrometric precision is driven by the desire to achieve a proper motion accuracy of 0.2 mas/yr and parallax accuracy of 1.0 mas over the course of the survey. These two requirements correspond to relative astrometric precision for a single image of 10 mas (per coordinate).

About 25% of blue stars ($g - r < 1$) and 50% of red stars brighter than $r = 20$ have proper motions greater than 10 mas/yr. Thus, to verify that these requirements are met, it may be necessary to use quasars, which have a sky surface density of about 60 per square degree for $r < 20$ (implying a mean separation of $\sim$4 arcmin).

Quantity	Design Spec	Minimum Spec	Stretch Goal
AM1 (milliarcsec)	10	20	5
AF1 (%)	10	20	5
AD1 (milliarcsec)	20	40	10
AM2 (milliarcsec)	10	20	5
AF2 (%)	10	20	5
AD2 (milliarcsec)	20	40	10
AM3 (milliarcsec)	15	30	10
AF3 (%)	10	20	5
AD3 (milliarcsec)	30	50	20

Table 18: The specifications for astrometric precision. The three blocks of values correspond to D=5, 20 and 200 arcmin, and to astrometric measurements performed in the r and i bands.

Specification: The astrometric reference frame for an image obtained in a band other than r will be mapped to the corresponding r band image such that the rms of the distance distribution between the positions on the two frames will not exceed AB1 milliarcsec (for a large number of bright sources). No more than ABF1 % of the measurements will deviate by more than AB2 milliarcsec from the mean. The dependence of the distance between the positions on the two frames on the source color and observing conditions will be explicitly included in the astrometric model (Table 19).

Quantity	Design Spec	Minimum Spec	Stretch Goal
AB1 (milliarcsec)	10	20	5
ABF1 (%)	10	20	5
AB2 (milliarcsec)	20	40	10

Table 19: The requirements on the band-to-band astrometric transformation accuracy (per coordinate in arbitrary band, relative to the r band reference frame).

The requirements on the band-to-band astrometric transformation accuracy are driven by the detection of moving objects, de-blending of complex sources, and astrometric accuracy for sources detected in a single-band (*e.g.* high-redshift quasars detected only in the y band).

The absolute astrometry
Specification: The LSST astrometric system must transform to an external system (*e.g.* ICRF extension) with the median accuracy of AA1 milliarcsec (Table 20).

The accuracy of absolute astrometry is driven by the linkage and orbital computations for solar system objects. A somewhat weaker constraint is also placed by the need for positional cross-correlation with external catalogs. Note that the delivered absolute astrometric accuracy may be fundamentally limited by the accuracy of astrometric standard catalogs.

Quantity	Design Spec	Minimum Spec	Stretch Goal
AA1 (milliarcsec)	50	100	20

Table 20: The median error in the absolute astrometric positions (per coordinate, in milliarcsec).

Auxiliary System Characteristics

The weak lensing science may be jeopardized by systematics in shape measurements. The effects of ghosting, which can also contribute to systematics in the shape measurements, are partially addressed through photometric requirements (*e.g.* the fraction of objects with substandard photometry). The presence of ghost images which can be confused with new point sources and thus be a source of false transient detections must be minimized. Further constraints, such as maximum sensor area loss and up/down time, are addressed in the LSST System Requirements Document.

3.4   The Full Survey Specifications

By obtaining numerous images of the same area on the sky, LSST will be able to significantly extend the scientific reach of the single images described above. The required total number of images depends on each particular science program. Studies of LSST science capabilities performed to date have demonstrated that:

1. It is possible to design a "universal cadence" that would result in a common database of observations to be used by all science programs (see Appendix B).

2. The required survey lifetime is of the order 10 years. The strongest constraints on this lower limit come from the required number of images to perform robust weak lensing analysis and from the minimum time baseline to obtain sufficiently accurate proper motion measurements. A somewhat less quantitative constraint on the upper limit for the survey lifetime comes from the desire to avoid "stale science" and to stay at the technological forefront.

As a result of these studies, the adopted baseline design (see Appendix A) assumes a nominal 10-year duration with about 90% of the observing time allocated for the main LSST survey. The same assumption was adopted here to derive the requirements described below. Only visits that satisfy the requirements listed in the previous section are counted towards the specifications listed in this Section. For example, if the photometric accuracy falls below requirements due to complex atmospheric cloud structure, or due to extraneous noise sources inside the system, the data will not be counted. The remaining 10% of observing time will be used to obtain improved coverage of parameter space such as very deep ($r \sim 26$) observations, observations with very short revisit times ($\sim$1 minute), and observations of "special" regions such as the Ecliptic, Galactic plane, and the Large and Small Magellanic Clouds. A third type of survey, micro-surveys, that would use about 1% of the time, may also be considered.

Note that some quantities relevant for science analysis are indirectly defined. For example, while the accuracy for photometric redshifts is not specified, it is one of the main drivers for the bandpass selection, required photometric accuracy per single visit, and the number of visits. Simulations show that the requirements described here will result in photometric redshift accuracy in the range 1-3% (fractional rms for 1+z over the redshift range 0.2-3.0, the fraction of catastrophic failures is still being investigated; also, a training sample of galaxies with spectroscopic redshift may be needed in order to limit systematic errors). This performance is consistent with the level required by the science drivers. Unlike photometric redshifts whose accuracy is not very sensitive to the distribution of visits in time, the proper motion and parallax accuracies can significantly deteriorate for some types of cadence strategies. Therefore, the requirements for the proper motion and parallax accuracies are explicitly listed.

The sky area and distribution of visits vs. bandpass for the main survey

Detailed simulations show that, during its nominal 10-year lifetime, LSST will be capable of obtaining over 2,500,000 10 deg^2 visits (using exposure time of 2x15 seconds). Assuming an effective sky area of 20,000 deg^2 (less than the maximum observable area from a given site because of airmass constraints), this implies that each position on the sky can be visited about 1000 times (ignoring field overlaps). The distribution of these visits among the bandpasses (filters) will have a direct impact on the science of the full LSST survey.

The r and i bands should be preferentially selected over other bands because they will be used for shape measurements. Other bands cannot be neglected, however, because a broad wavelength coverage is required to achieve desired photometric redshift accuracy for galaxies and needed color information on transients such as supernovae. The impact of the visit distribution across bands can be gauged from the following two cases. If all 1000 visits were assigned equally to the r and i bands, their final depth, assuming $\sqrt{N}$ scaling, would be 3.4 mag deeper than the single image depth (see §3.3.2). If the visits were distributed equally over 6 bands, then the final depth would be 2.8 mag deeper than the single image depth. Note that the depth difference between these two scenarios is only 0.6 mag.

Detailed simulations of LSST operations indicate that the following sky coverage and allocation of observing time per band satisfies a variety of science drivers at a nearly optimal level. However, *the listed requirements should be understood only as an illustration of the LSST capabilities because the survey optimization is still in progress.*

Specification: The sky area uniformly covered by the main survey will include Asky square degrees (Table 21).

Quantity	Design Spec	Minimum Spec	Stretch Goal
Asky (deg^2)	18,000	15,000	20,000

Table 21: The sky area uniformly covered by the main survey.

The design specification for the sky area uniformly covered by the main survey is a result of maximizing the number of galaxies detected at a fiducial signal-to-noise ratio,

given a fixed total exposure time. The derived area corresponds to an airmass limit of 1.4 (including accounting for the Galactic plane area and variable observing conditions), which assures that the delivered image size degradation as a function of airmass is not larger than the degradation induced by the system (see Table 9), and that the image depth degradation due to increased airmass is not larger than variations due to varying sky brightness.

Specification: The sum of the median number of visits in each band, Nv1, across the sky area specified in Table 21, will not be smaller than Nv1 (Table 22).

Quantity	Design Spec	Minimum Spec	Stretch Goal
Nv1	825	750	1000

Table 22: The sum of the median number of visits in each band across the sky area specified in Table 21.

An illustration of the distribution of Nv1 is shown in Table 23. It is assumed that $\sim$10% of the total observing time is allocated to each of the u and g bands, and $\sim$20% to each of the $rizy$ bands. These allocations reflect the dependence of the desired final coadded depths on bandpass, as well as a minimum number of visits in the r and i bands to enable exquisite control of image shape systematics. The bandpass dependence of the coadded depths is optimized using a mean galaxy spectral energy distribution at a redshift of $\sim$2. The adopted depths are also well matched to spectral energy distributions of blue stars (main sequence stars will enable kinematic and metallicity studies all the way to the presumed edge of the Milky Way halo) and low-redshift quasars, and to those of very red objects (e.g., high-redshift quasars and galaxies, the coldest stars, highly reddened stars in the Milky Way disk). The simulations assume an exposure time of 30 seconds per visit, which is a result of the survey optimization using *simultaneous* constraints for the single visit depth, the number of visits, the revisit time, and the surveying efficiency (see Section 2.2 in the LSST overview paper, arXiv:0805.2366).

The coadded image depth losses due to airmass greater than unity are not taken into account because they depend on cadence details. For a large suite of simulated main survey cadences, they are about 0.2-0.3 mag, with the median airmass in the range 1.2-1.3. Table 23 specifies the *median* number of visits. The actual number of visits may vary across the sky. For example, the regions close to the Ecliptic may benefit from longer exposures to improve the size and distance limit for distant solar system objects. These regions may also require a larger than median number of visits to improve the completeness level for small asteroids. On the other hand, the Galactic plane regions may have smaller than median number of visits (*e.g.* very deep images may be confusion limited). Details of such variations are not specified here, with an understanding that *the adopted observing strategy will not jeopardize the goals of any of the four main science themes* (*e.g.* the full avoidance of the Galactic plane would have a severe impact on the Galactic structure studies). For the same reason, minimum specification and stretch goal values per band are also not specified. The median total number of visits (824 here) is expected to be uncertain by about 10% due to unpredictable observing conditions and details of the final adopted observing strategy.

Quantity	u	g	r	i	z	y
Nv1 (design spec.)	56 (2.2)	80 (2.4)	184 (2.8)	184 (2.8)	160 (2.8)	160 (2.8)
Idealized Depth	26.1	27.4	27.5	26.8	26.1	24.9

Table 23: An *illustration* of the distribution of the number of visits as a function of band-pass, obtained by detailed simulations of LSST operations that include realistic weather, seeing and sky brightness distributions, as well as allocation of about 10% of the total observing time to special programs. The median number of visits per field for all bands is 824. For convenience, the numbers in parentheses show the corresponding gain in depth (magnitudes), assuming $\sqrt{N}$ scaling. The last row shows the total *idealized* coadded depth for the design specification median depth of a single image (assuming 5σ depths at $X = 1$ of $u = 23.9$, $g = 25.0$, $r = 24.7$, $i = 24.0$, $z = 23.3$ and $y = 22.1$, from Table 6), and the above design specification for the total number of visits. The coadded image depth losses due to airmass greater than unity are not taken into account. For a large suite of simulated main survey cadences, they are about 0.2-0.3 mag, with the median airmass in the range 1.2-1.3.

Distribution of visits in time

The LSST will be capable of observing 20,000 deg^2 of the sky in two bands every three nights. While the data obtained with such a cadence will contribute greatly to studies of optical transients, it is desirable to explore much shorter scales, down to 1 minute. This can be achieved with frequent revisits to the same field, or by utilizing field overlap. The details of the revisit time distribution, and its dependence on the covered area, will greatly depend on the adopted observing strategy and here only rough guidance is provided.

Specification: At least RVA1 square degrees will have multiple observations separated by nearly uniformly sampled time scales ranging from 40 sec to 30 min (Table 24).

Quantity	Design Spec	Minimum Spec	Stretch Goal
RVA1 (deg^2)	2,000	1,000	3,000

Table 24: The minimum area with fast (40 sec – 30 min) revisits.

The requirements are derived using the universal cadence described in Appendix B as a minimalistic scenario. It shows that $\sim$10% of the total area can be revisited on short time scales by utilizing field overlaps.

Strong constraints on the distribution of visits in time come from the goal of accurately measuring stellar parallax and proper motion (see Section 2.4). Irrespective of the delivered astrometric precision, parallax measurements will not be of sufficient accuracy if the majority of visits are clustered around the same epoch. Similarly, proper motion measurements require that a large fraction of the observations are spread over as long a baseline as possible.

Specification: The median trigonometric parallax accuracy across the main survey area for unresolved sources with $r = 24$ must be at least SIGpara mas. The median proper

motion accuracy per coordinate across the main survey area for such sources must be at least SIGpm The median trigonometric parallax accuracy across the main survey area for unresolved sources detected only in the y band (at 10σ) must be at least SIGparaRed mas. (Table 25).

Quantity	Design Spec	Minimum Spec	Stretch Goal
SIGpara (mas)	3.0	6.0	1.5
SIGpm (mas/yr)	1.0	2.0	0.5
SIGparaRed (mas)	6.0	10.0	3.0

Table 25: The required trigonometric parallax and proper motion accuracy.

These requirements constrain the distribution of visits in time and are derived from the requirements for proper motion accuracy of 0.2 mas/yr at $r = 20.5$, trigonometric parallax accuracy of 1 mas at $r = 22.4$, and trigonometric parallax accuracy of 6 mas for red sources with only 10σ y-band detections, per Section 2.4. Detailed simulations show that the baseline cadence can deliver this performance for main sequence stars (Section 3.3.3 in the LSST overview paper, arXiv:0805.2366), if the astrometric requirements from the previous section are met.

Additional constraints on the distribution of visits in time come from the requirement to efficiently detect and characterize moving Solar System objects. In addition to their own science drivers, this requirement is driven by the fact that they may significantly contaminate samples of transients (see Section 2.3). In order to enable robust inter-night linking of their detections, the current baseline cadence assumes two visits per night (see Appendix B).

Distribution of visits vs. observing conditions

Observing conditions include, but are not limited to, seeing, sky brightness (affected by lunar phase and time of night), transparency, and airmass. Designing a cadence which will optimize performance on the mixed science goals described in this document will necessarily involve some compromises between conflicting goals. The algorithm employed by the observation scheduler will balance these goals, take advantage of current conditions, and maintain as uniform coverage as possible in both time and location on the sky.

It is assumed that the observing strategy will follow standard practices as much as possible when selecting the bandpass and sky location of a particular visit (*e.g.* blue exposures should preferentially take place around the new moon, and bright time observations will avoid the moon as much as possible). However, for some transient science, especially high-redshift supernovae, it is critical to sample the z and y bands throughout the light-curve, and this will necessitate altering these standard practices to some extent. Weak lensing science mandates that the r and i band observations be performed in the best seeing nights, and at low airmass. It also requires a large range of angles between the pupil, detector, and sky to minimize possible systematic errors.

The overall image PSF ellipticity distribution

A limit to the effectiveness of the PSF-correction schemes is our knowledge of the delivered PSF within each image, which is sampled at high Galactic latitude roughly three times per square arcminute by a high S/N ratio star and must be interpolated at the positions of the galaxies. (There is a color dependence, such that the stellar PSF must also be interpolated to the colors of the galaxies, but we do not address that issue here.)

To address these systematics, we first define ellipticity components

$$e_1 = \frac{\sigma_1^2 - \sigma_2^2}{\sigma_1^2 + \sigma_2^2}, \tag{10}$$

and

$$e_2 = \frac{2\sigma_{12}^2}{\sigma_1^2 + \sigma_2^2}, \tag{11}$$

where σ_1^2 and σ_2^2 are the 2nd moments of the stellar image along some set of perpendicular axes, and σ_{12}^2 is the covariance (again, for the best-fit elliptical Gaussian). A PCA fit to the ellipticity components dependence on the position within each CCD is made, and we examine the residuals. It is the *correlation of these residuals* δe_1 and δe_2, not their mean size, which sets the level of weak lensing systematics. We define the residual ellipticity auto and cross correlation functions

$$E_1(\theta) = \langle \delta e_1^{(i)} \delta e_1^{(j)} \rangle, \tag{12}$$

$$E_2(\theta) = \langle \delta e_2^{(i)} \delta e_2^{(j)} \rangle, \tag{13}$$

and

$$E_X(\theta) = \langle \delta e_1^{(i)} \delta e_2^{(j)} \rangle, \tag{14}$$

where angle brackets indicate averaging over all pairs of stars i and j at a given angular separation θ. Again, we use the natural limit of the atmosphere as a guide. Observations indicate that the residuals E_1, E_2, and E_X are $\sim 10^{-4}$ at scales of an arcminute and smaller for a 10-second exposure at 0.7 arcsec delivered seeing, falling below shot noise levels at $\theta = 5$ arcmin. It is a requirement that LSST images not degrade this quality significantly. The defocus spectrum from atmosphere induced seeing, combined with optics astigmatism and FPA (focal plane array) non-flatness, produces so-called "B mode" shear (non-zero E_X). Using as priors the measured FPA non-flatness, the wavefront curvature measurements for that image, and the optics astigmatism vs. defocus data, one can optimally fit the PSF over the image. Similarly, requirements on these instrument parameters can be deduced from the science requirements on the residual ellipticity correlations.

Specification: Using the full survey data, the E_1, E_2, and E_X residual PSF ellipticity correlations averaged over an arbitrary FOV must have the median less than TE1 for $\theta \leq 1$ arcmin, and less than TE2 for $\theta \geq 5$ arcmin. No more than TEF % of images will have these medians larger than TE3 for $\theta \leq 1$ arcmin, and TE4 for $\theta \geq 5$ arcmin (Table 26).

The residual ellipticity correlations vary smoothly so it is sufficient to specify limits in these two angular ranges. On 1 arcmin to 5 arcmin scales, these residual ellipticity

Quantity	Design Spec	Minimum Spec	Stretch Goal
TE1	2×10^{-5}	3×10^{-5}	1×10^{-5}
TE2	1×10^{-7}	3×10^{-7}	5×10^{-8}
TEF	15%	15%	10%
TE3	4×10^{-5}	6×10^{-5}	2×10^{-5}
TE4	2×10^{-7}	5×10^{-7}	1×10^{-7}

Table 26: These residual PSF ellipticity correlations apply to the r and i bands.

correlations put LSST systematics a factor of a few below the weak lensing shot noise, i.e. statistical errors will dominate over systematics. On larger scales, the noise level imposed by nature due to shot noise plus cosmic variance is almost scale-independent, whereas the atmospheric contribution to systematics becomes negligible. Therefore the specifications on 5 arcmin scales apply to all larger scales as well (as per section 2.1.1). On scales larger than the field of view, sources of systematic error have less to do with the instrumentation than with the operations (due to the seeing distribution), software, and algorithms. It is recommended that the scheduler attempt to match the seeing distribution in each patch of sky, so that at the end of the survey at most a small fraction of patches will have substantially better or worse seeing than average.

3.5   Data Processing and Management Requirements

Detailed requirements on data processing and management will be described in the LSST System Requirements Document (for example, specifications for catalog completeness and reliability). Here, only a rough guidance is provided. There will be three main categories of data products:

- **Level 1** data products are generated continuously every observing night, including alerts to objects that have changed brightness or position.

- **Level 2** data products will be made available as annual Data Releases and will include images and measurements of positions, fluxes, and shapes, as well as variability information such as orbital parameters for moving objects and an appropriate compact description of light curves.

- **Level 3** data products will be created by science teams external to the project using suitable Applications Programming Interfaces (APIs) that will be provided by the LSST Data Management System. The Data Management System will also provide at least 10% of its total capability for user-dedicated processing and user-dedicated storage. The key aspect of these capabilities is that they will reside "next to" the LSST data, avoiding the latency associated with downloads. They will also allow the science teams to use the database infrastructure to store their results.

Specification: Images and catalog data will be released to publicly-accessible repositories as soon as possible after they are obtained. This latency, and the exact form of the

data to be continuously released, are left unspecified at this time pending further discussion within the project. Data on likely optical transients, however, will be released with a latency of at most OTT1 minutes.

Acknowledging that science thrives on repeatability of results, however, it is recognized that specific, fixed "snapshots" of the data should periodically be released so that data used in published analyses can unambiguously be referenced. The object catalogs in these snapshot data releases will include an extensive list of measured properties that will allow a variety of science analyses without the need to reprocess images. These catalogs and images, corrected for instrumental artifacts, and photometrically and astrometrically calibrated, will be released to public every DRT1 years (Table 27). The catalogs and images will be released for both single visits and for appropriately co-added data (such as those optimized for depth and for weak lensing analysis). The catalog data in these releases may be more extensive (*i.e.* reflect more analysis) than that released on a continuing basis. The catalogs will be released in a format that will allow efficient data access and analysis (such as a database and query system).

Quantity	Design Spec	Minimum Spec	Stretch Goal
DRT1 (year)	1.0	2.0	0.5
OTT1 (min)	1.0	2.0	0.5

Table 27: Requirements for the data release cadence and for the transient reporting latency.

The requirement on the data release cadence is a compromise between "too often", which may have an impact on the system's efficiency, and "too slow", which may have an impact on the system's science outcome and its perception within the community. The requirement on the transient reporting latency is essentially driven by the total exposure time, which sets an intrinsic scale for the time resolution of transient sources.

The fast release of data on likely optical transients will include measurements of position, flux, size and shape, using appropriate weighting functions, for all the objects detected above transSNR signal-to-noise ratio in difference images (design specification: 5). The data stream will also include prior variability information and data from the same night, if available. The prior variability information will at the very least include low-order light-curve moments and probability that the object is variable, and ideally the full light curves in all available bands.

Specification: The system should be capable of reporting such data for at least transN candidate transients per field of view and visit (Table 28).

Quantity	Design Spec	Minimum Spec	Stretch Goal
transN	10^4	10^3	10^5

Table 28: The minimum number of candidate transients per field of view that the system can report in real time.

The users will have an option of a query-like pre-filtering of this data stream in order to select likely candidates for specific transient type. Users may also query the LSST science database at any time for additional information that may be useful, such as the properties of static objects that are positionally close to the candidate transients. Several pre-defined filters optimized for traditionally popular transients, such as supernovae and microlensed sources, will also be available, as well as the ability to add new pre-defined filters as the survey continues.

3.6   Further Improvements and Changes

A number of LSST-related design and scientific studies are under way that may affect the requirements described in this document. In addition, it is quite possible that further specifications may be requested during the process of distilling this document into the LSST Engineering Requirements Document. Any such changes to this document will need to be brought to the attention of the LSST Science Council, who will review the case and, if appropriate, propose changes to the LSST Change Control Board. Please report such, and any other, concerns and comments to Željko Ivezić[7].

4   Authorship

This document is the result of deliberations by the members of LSST Science Council, listed below, who also benefitted greatly from input from a variety of people, including, but not restricted to: Neil Brandt, Kem Cook, Gregory Dubois-Felsmann, Daniel Eisenstein, Peter Garnavich, Perry Gee, Richard Green, Alan Harris, Lynne Jones, Tod Lauer, Jeremy Mould, Knut Olsen, Steve Ridgway, Abi Saha, Don Schneider, Mike Shara, Chris Smith, Nick Suntzeff, David Wittman, Sidney Wolff, and Dennis Zaritsky.

The members of the LSST Science Council are: Tim Axelrod, David Burke, Chuck Claver, Andy Connolly, Kirk Gilmore, Željko Ivezić (chair), Steve Kahn, Robert Lupton, Dave Monet, Phil Pinto, Michael Strauss, Chris Stubbs, Don Sweeney (ex officio), Alex Szalay, and Tony Tyson (ex officio).

---

[7]E-mail: ivezic@astro.washington.edu

Appendix A: The LSST Baseline Design

The following tables includes excerpts from the March 16, 2010 LSST Baseline Design Summary (available from http://www.lsst.org/lsst/science/survey_requirements) that are most relevant to this document.

Excerpts from the Baseline Design Summary

Quantity	Baseline Design Specification
Optical Configuration	3-mirror modified Paul-Baker
Mount configuration	Alt – Azimuth
Final f-Ratio	f/1.234
Field of view area	9.6 deg^2
Aperture	8.4 m
Effective aperture	6.68 m
Effective étendue (AΩ)	319 m^{2}deg^2
Plate Scale	50.9 microns/arcsec (0.2 arcsec pix)
Pixel count	3.2 Gigapixel
Wavelength Coverage	330 – 1070 nm
Standard exposure sequence	41 sec total for 2x15 sec exposure (with slew, without filter change)

Table 29: The LSST March 2010 Baseline Design Parameters.

Appendix B: The Universal Cadence Strategy

Strict optimization of each of the numerous science programs that LSST will enable would certainly result in the same number of observing strategies. However, thanks to the large étendue, it is possible to design a universal cadence that would result in a common database of observations to be used by all science programs. An example of such a cadence is described here and presented as a "proof of concept" rather than as a specific requirement on the observing strategy. It does not address the possibility of deeper, or more frequent, KBO and SNe surveys discussed in §3.4.

This, so-called "universal cadence", has a number of desirable properties, and in particular, samples a wide range of time scales that are necessary for time domain science. Equally important, the proposed cadence is invariant to time translation and reversal, a feature that is desirable for a massive steady-state synoptic sky survey. More details about this proposal are available in the LSST Science Working Group report, and here only its essential characteristics are described.

The strategy proposes two revisits closely separated in time (15-60 min) to enable a robust and simple method for linking main-belt asteroids (MBA). Their sky surface density is about two orders of magnitude higher than the expected density of potentially hazardous asteroids (PHA), and thus MBAs must be efficiently and robustly recognized in order to find PHAs. MBAs move about 3-18 arcmin in 24 hours, which is larger than their typical nearest neighbor distance at the depths probed by LSST (2.3 arcmin on the Ecliptic). Two visits closely separated in time enable linking based on a simple search for the nearest moving neighbor, with a false matching rate of only a few percent.

With this cadence, it is possible to observe 20,000 deg^2 of sky in about three nights, with two visits per field. The colors of transients (such as SNe) and moving objects can also be measured by using two different filters for the two visits (with a preference given to the r band).

Due to the proposed overlap between successive fields of view, about 17% of the observed area represent multiple observations with a variety of time scales. With a representative choice of various free parameters, about 5% of the observed area would be revisited within 25 sec. Another 10% of the area would be reobserved with a fairly uniform sampling of time scales ranging from 25 sec to 15 min.
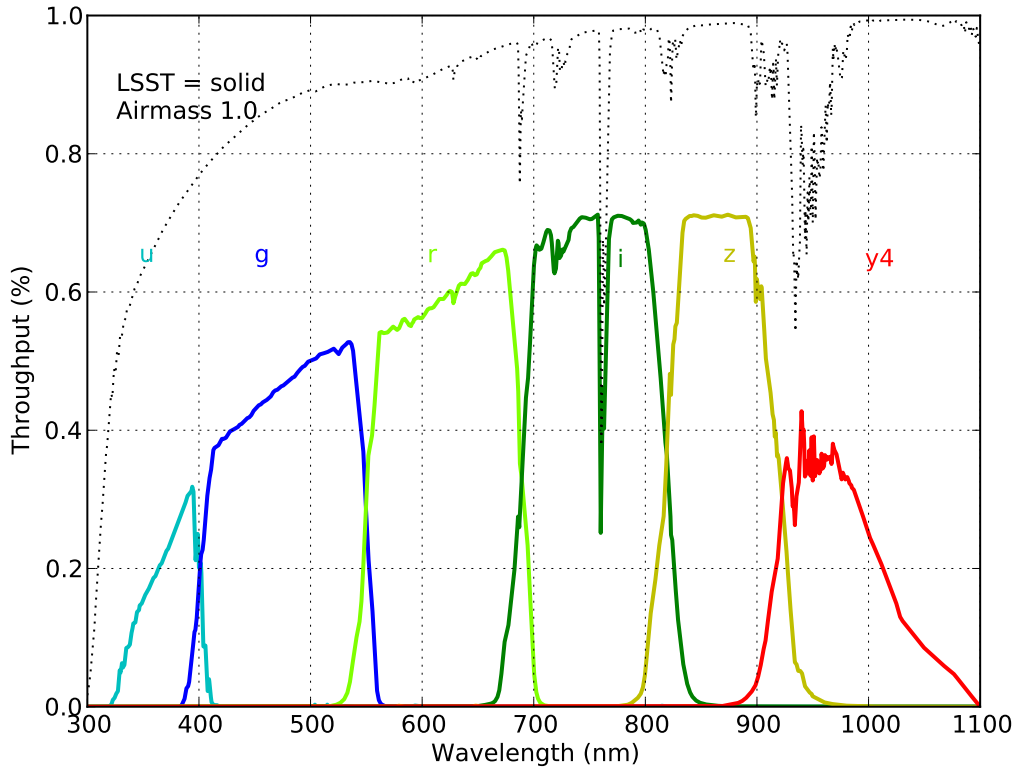
Appendix C: The LSST Bandpasses

Figure 1: The *current* design of the LSST bandpasses (solid lines: the full throughput, including the atmosphere and idealized system, described by $S_b(\lambda)$ from eq. 6). The dotted line shows the throughput for a standard atmosphere at airmass $X = 1.0$ used in computations ($S^{atm}(\lambda)$ from eq. 6).

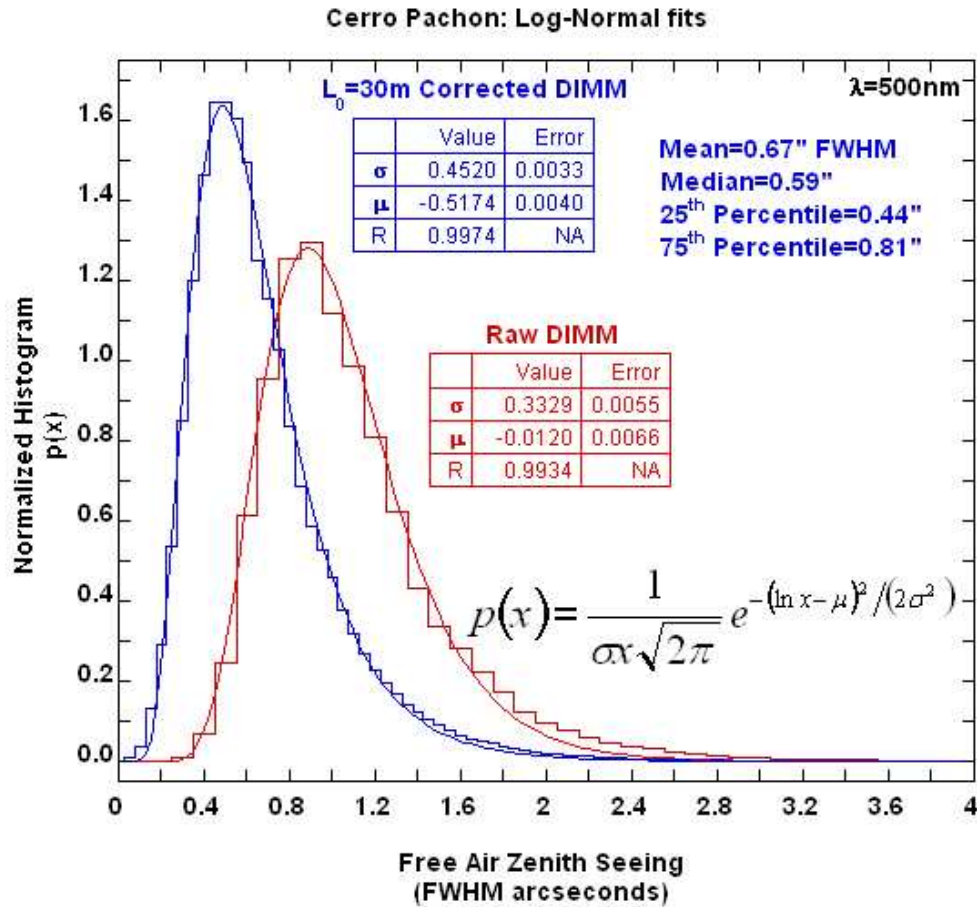# Appendix D: The Seeing Distribution at the Cerro Pachón site

Figure 2: The seeing distribution measured at the Cerro Pachón site using DIMM at 500 nm (red histogram), and corrected using the outer scale parameter of 30 m (blue histogram). For details about the outer scale correction see Tokovinin 2002 (PASP, 114, 1156). The lines show best-fit log-normal distributions, with the best-fit parameters as shown in the inset (computed by C. Claver).

Appendix E: The Document History

1. **Version 4.3 (September 2007)** The first version approved by the LSST Board, placed under the Change Control Board, and made public.

2. **Version 5.1 (May 2010)** The most important changes, relative to v4.3, are:

   - Incorporated references to the LSST Science Book
   - Made listed science drivers normative
   - Listed expected performance for photometric redshifts of galaxies
   - Improved quantitative drivers and specifications for trigonometric parallax and proper motion
   - Adopted a general principle that software algorithms should not dominate measurement errors
   - Relaxed minimum requirements for single-image depth (by 0.2-0.3 mag)
   - Made it explicit that the system throughput function is a part of photometric data products
   - Removed specifications for ghosting
   - Removed specifications for modeling residuals for single-image ellipticity
   - Made explicit mini and micro surveys
   - Made explicit the three levels of data products

Parameters Specified in this Document

AA1

The median accuracy of the astrometric transformation from the LSST system to an external system (milliarcsec). p. 24

AB1

The maximum rms distance between images in r and in other bands (milliarcsec). p. 24

AB2

At most ABF1 % of rms distances between images in r and in other bands will be greater than this value (milliarcsec). p. 24

ABF1

The maximum fraction of rms distances between images in r and in other bands greater than AB2 (see AB1)(%). p. 24

ADx

AFx of the astrometric distances will deviate by more than this (see AMx, AFx) (milliarcsec). p. 23

AFx

The maximum fraction of astrometric distances which deviate by more than ADx milliarcsec (see AMx) (%). p. 23

AMx

The maximum rms of the astrometric distance distribution for stellar pairs with separations of D arcmin (repeatability) (x=1,2,3 → D=5, 20, 200 arcmin) (milliarcsec). p. 23

Asky

The sky area uniformly covered by the main survey. p. 26

D1

The brightest median 5σ (SNR=5) detection depth for point sources for all exposures in a given band (mag). p. 14

DB1

The median 5σ (SNR=5) detection depth for point sources for all exposures in a given band (mag). p. 14

DF1

The fraction of images with 5σ depth brighter than parameter Z1 (%). p. 14

DF2

The maximum fraction of images Z2 mag brighter than the median depth over individual devices (%). p. 15

DRT1

The maximum interval between public releases of "snapshot" catalog and image data (years). p. 32

EF1

The maximum fraction of ellipticities exceeding an ellipticity of SE2 (%). p. 19

ETmin

The minimum required exposure time (sec). p. 16

Fleak

The maximum permitted out-of-band flux for filters (defined as flux, normalized by the peak value, in any 10nm interval at wavelengths beyond those where the transmission curve decreases to below 0.1% of its peak value for the first time) (%). p. 13

FleakTot

The maximum integrated out-of-band filter transmission at all wavelengths beyond those where the transmission curve decreases to below 0.1% of its peak value for the first time (%). p. 13

Nfilters

The number of filters that can be housed simultaneously within the camera. p. 12

Nv1

The median of the distribution of the number of visits across the sky in a given band. p. 27

OTT1

The minimum latency for releasing data on optical transients (minutes). p. 32

PA1

The maximum rms of the unresolved source magnitude distribution around the mean value (repeatability) (millimag). p. 21

PA2

At most PF1 % of magnitudes may deviate by more than this from the mean (millimag). p. 21

PA3

The maximum rms of the internal photometric zero-point error (the system stability across the sky) (millimag). p. 21

PA4

At most PF2 % of internal photometric zeropoint errors may exceed this value (millimag). p. 21

PA5

Color zero-points for main-sequence stars must be known to this accuracy (millimag). p. 22

PA6

The transformation from the LSST photometric system to a physical scale must be at least this accurate (millimag). p. 22

PF1

The maximum fraction of magnitudes deviating by more than PA2 from mean (%). p. 21

PF2

The maximum fraction of internal photometric zero-point errors exceeding PA4 (%). p. 21

pixSize

The maximum pixel size (arcsec). p. 18

RVA1

The minimum area of sky with multiple observations separated by nearly uniformly sampled time scales ranging from 40 sec to 30 min (square degrees). p. 28

S1

The maximum delivered median seeing (arcsec). p. 17

SE1

The maximum median ellipticity across the field of view for unresolved sources (ellipticity). p. 19

SE2

EF1 % of the ellipticities may exceed this value (see EF1) (ellipticity). p. 19

SF1

The maximum fraction of images with median seeing exceeding S1∗SX arcsec (see S1, SX) (%). p. 17

SIGpara

The trigonometric parallax error for a $r=24$ source (mas). p. 28

SIGparaRed

The trigonometric parallax error for 10σ y-band only detections (mas). p. 29

SIGpm

The proper motion error for a $r=24$ source (mas/yr). p. 29

SR1

The 80% encircled energy diameter for median seeing (arcsec). p. 18

SR2

The 90% encircled energy diameter for median seeing (arcsec). p. 18

SR3

The 99% encircled energy diameter for median seeing (arcsec). p. 18

SX

A scale factor on S1 used in defining SF1 (see S1, SF1). p. 17

SXE

The allowed error budget due to system at airmass=2 (arcsec). p. 17

TE1

The maximum value for the median ellipticity correlation function on ≤ 1 arcmin scale for unresolved bright sources using the full survey data (hereafter ellipticity). p. 30

TE2

The maximum value for the median ellipticity correlation function on ≥ 5 arcmin scale for unresolved bright sources using the full survey data (hereafter ellipticity). p. 30

TE3

At most TEF % of ellipticities for unresolved bright sources using the full survey data may exceed this value on ≤ 1 arcmin scales (see TE1). p. 30

TE4

> At most TEF % of ellipticities for unresolved bright sources using the full survey data may exceed this value on ≥5 arcmin scales (see TE3). p. 30

TEF

> The maximum fraction of ellipticities for unresolved bright sources using the full survey data exceeding TE3 or TE4 (%). p. 30

TFmax

> The maximum time allowed to switch filters already present inside the camera (minutes). p. 13

transN

> The minimum number of candidate transients per field of view that the system can report in real time p. 32

transSNR

> The minimum signal-to-noise ratio in difference image for reporting detection of a transient object p. 32

Z1

> DF1 % of images will have a depth brighter than this value (used to describe the tail of the distribution) (mag) (see DF1). p. 14

Z2

> DF2 % of images on different devices will be this much brighter than the median depth (mag) (see DF2). p. 15